# A New Form of Fluxional Process in the Sterically Hindered Oxo Cluster $[Ru_3(\mu_3\text{-}O)(\mu_3\text{-}CO)(CO)_3(\mu\text{-}Ph_2PCH_2PPh_2)_3]$

**Hameed A. Mirza, Jagadese J. Vittal, and Richard J. Puddephatt***

Department of Chemistry, University of Western Ontario, London, Canada N6A 5B7

*Received December 15, 1994*[⊗]

Oxidation of $[Ru_3(CO)_6(\mu\text{-dppm})_3]$, dppm = $Ph_2PCH_2PPh_2$, by silver(I) and $O_2$ or $Me_3NO$ gives the oxo cluster complex $[Ru_3(\mu_3\text{-}O)(\mu_3\text{-}CO)(CO)_3(\mu\text{-dppm})_3]$, **3**, which can undergo reversible protonation to give the related hydroxo cluster $[Ru_3(\mu_3\text{-}OH)(\mu_3\text{-}CO)(CO)_3(\mu\text{-dppm})_3]^+$. The structure of **3** has been determined [monoclinic, $P2_1/n$, $a$ = 19.771(2) Å, $b$ = 29.711(2) Å, $c$ = 13.007(2) Å, $\beta$ = 94.01(9)°, $V$ = 7622(1) Å$^3$, $Z$ = 4, $R_F$ = 0.063]. These clusters are sterically congested and exhibit an interesting new form of fluxionality in clusters based on the $M_3(\mu\text{-dppm})_3$ unit.

## Introduction

There is continuing interest in organometallic complexes of late transition metals containing oxo ligands since they can serve as models for intermediates in catalytic oxidation or as reagents or catalysts in oxidation of organic compounds.[1-5] Polynuclear oxo complexes are of particular interest as they may provide a link between organometallic oxides and inorganic oxides or polyoxyanions.[3] This paper reports the synthesis and characterization of an oxo triruthenium cluster $[Ru_3(\mu_3\text{-}O)(\mu_3\text{-}CO)(CO)_3(\mu\text{-dppm})_3]$, dppm = $Ph_2PCH_2PPh_2$, and the related hydroxo cluster $[Ru_3(\mu_3\text{-}OH)(\mu_3\text{-}CO)(CO)_3(\mu\text{-dppm})_3]^+$. These clusters are sterically congested and exhibit an interesting new form of fluxionality in clusters based on the $M_3(\mu\text{-dppm})_3$ unit.

## Results and Discussion

**Synthesis of the Oxo Cluster 3.** Earlier we reported the structures of the cluster $[Ru_3(CO)_6(\mu\text{-dppm})_3]$, **1**, and the product of its protonation $[Ru_3(\mu\text{-}H)(CO)_6(\mu\text{-dppm})_3]^+$, **2**.[6] In an attempt to make an isolobal analog of **2**, the cluster **1** in solution in dichloromethane was reacted with silver(I) trifluoroacetate in ethanol, using an atmosphere of air. The unexpected product was an orange-yellow cluster identified as $[Ru_3(\mu_3\text{-}O)(\mu_3\text{-}CO)(CO)_3(\mu\text{-dppm})_3]$, **3**. During the reaction, a silver mirror was deposited on the walls of the vessel. Subsequently, it was found that the reaction could be accelerated by addition of $Me_3NO$ to the mixture.

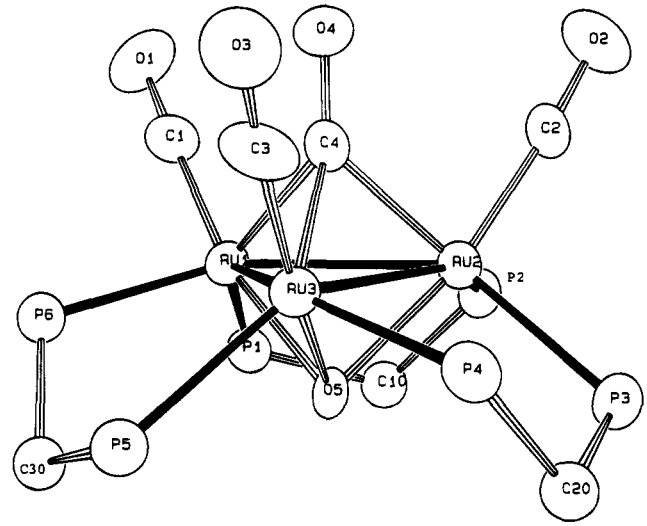


**Figure 1.** ORTEP diagram of the skeleton (50% probability thermal ellipsoids) along with the atom-numbering scheme. The phenyl rings are omitted for clarity.

**Structure of the Oxo Cluster 3.** A view of the structure of **3** is shown in Figure 1, and selected bond distances and angles are listed in Table 1. The cluster contains a triangle of ruthenium atoms with distances Ru–Ru from 2.727(1) to 2.747(1) Å. Each edge of the $Ru_3$ triangle is bridged by a dppm ligand. Above one face of the $Ru_3$ triangle, each ruthenium atom is coordinated by a terminal CO group and the fourth CO group is triply bridging, giving rise to a $Ru_3(\mu_3\text{-}CO)(CO)_3$ unit. The other face of the $Ru_3$ triangle contains the oxo ligand in a triply bridging coordination mode [Ru–O = 2.072(7)–2.084(7) Å]. The cluster has the 48-electron, closed-shell configuration with the $\mu_3$-O ligand contributing four electrons. The average Ru–Ru distance of 2.736 Å in **3** is significantly shorter than those in $[Ru_3(CO)_6(\mu\text{-dppm})_3]$ at 2.855 Å[6] or in $[Ru_3(CO)_{12}]$ at 2.854 Å,[7] while slightly longer than that in the related cluster $[Ru_3(\mu_3\text{-}O)(CO)_6(\mu\text{-dpam})_2]$, dpam = $Ph_2AsCH_2AsPh_2$, at 2.71 Å.[8] Thus, the $\mu_3$-oxo ligand appears to favor short Ru–Ru bonds.

[⊗] Abstract published in *Advance ACS Abstracts,* July 1, 1995.

(1) (a) Almog, O.; Bino, A.; Garfinkelshweky, D. *Inorg. Chim. Acta* **1993**, *213*, 99. (b) Angermaier, K.; Schmidbaur, H. *Inorg. Chem.* **1994**, *33*, 2069. (c) Ingham, S. L.; Lewis, J.; Raithby, P. R. *J. Chem. Soc., Chem. Commun.* **1993**, 166. (d) Park, J. T.; Chi, Y.; Shapley, J. R.; Churchill, M. R.; Ziller, J. W. *Organometallics* **1994**, *13*, 813. (e) Xiao, J.; Puddephatt, R. J.; Manojlovic-Muir, Lj.; Muir, K. W.; Torabi, A. A. *J. Am. Chem. Soc.* **1994**, *116*, 1129. (f) He, X.-D.; Chaudret, B.; Lahoz, F.; Lopez, J. A. *J. Chem. Soc., Chem. Commun.* **1990**, 958. (g) Voss, E. J.; Sabat, M.; Shriver, D. F. *Inorg. Chem.* **1991**, *30*, 2705 (h) Ceriotti, A.; Resconi, L.; Demartin, F.; Longoni, G.; Manassero, M.; Sansoni, M. *J. Organomet. Chem.* **1983**, *249*, C35. (i) Ciani, G.; Sironi, A.; Albano, V. G. *J. Chem. Soc., Dalton Trans.* **1977**, 1667.

(2) (a) Bartley, S. L.; Dunbar, K. R.; Shih, K. Y.; Fanwick, P. E.; Walton, R. A. *J. Chem. Soc., Chem. Commun.* **1993**, 98. (b) Budzichowski, T. A.; Chisholm, M. H.; Streib, W. E. *J. Am. Chem. Soc.* **1994**, *116*, 389. (c) Hoard, D. W.; Sharp, P. R. *Inorg. Chem.* **1993**, *32*, 612. (d) Li, J. J. J.; Sharp, P. R. *Inorg. Chem.* **1994**, *33*, 183.

(3) (a) Bottomley, F.; Boyle, P. D.; Chen, J. H. *Organometallics* **1994**, *13*, 370. (b) Herrmann, W. A. *J. Organomet. Chem.* **1986**, *300*, 111. (c) Legzdins, P.; Rettig, S. J.; Sanchez, L. *Organometallics* **1985**, *4*, 1479. (d) Klemperer, W. G.; Schwartz, C.; Wright, D. A. *J. Am. Chem. Soc.* **1985**, *107*, 6941.

(4) (a) Sheldon, R. A.; Kochi, J. K. *Metal-Catalyzed Oxidation of Organic Compounds*; Plenum: New York, 1981. (b) Drago, R. S. *Coord. Chem. Rev.* **1992**, *117*, 185. (c) Griffith, W. P. *Chem. Soc. Rev.* **1992**, 179. (d) Sawabe, K.; Matsumoto, Y. *Surf. Sci.* **1994**, *303*, L385.

(5) Bottomley, F.; Sutin, L. *Adv. Organomet. Chem.* **1988**, *28*, 339.

(6) Mirza, H. A.; Vittal, J. J.; Puddephatt R. J. *Inorg. Chem.* **1993**, *32*, 1327.

(7) Churchill, M. R.; Hollander, F. J.; Hutchinson, J. P. *Inorg. Chem.* **1977**, *16*, 2655.

0020-1669/95/1334-4239$09.00/0 

**Table 1.** Selected Bond Distances (Å) and Angles (deg)

| | | | |
|---|---|---|---|
| Ru(1)−Ru(2) | 2.727(1) | Ru(1)−Ru(3) | 2.733(2) |
| Ru(2)−Ru(3) | 2.747(1) | Ru(1)−P(1) | 2.342(4) |
| Ru(1)−P(6) | 2.294(3) | Ru(2)−P(2) | 2.294(4) |
| Ru(2)−P(3) | 2.379(3) | Ru(3)−P(4) | 2.275(3) |
| Ru(3)−P(5) | 2.381(3) | Ru(1)−C(1) | 1.81(1) |
| Ru(1)−C(4) | 2.08(1) | Ru(2)−C(2) | 1.82(1) |
| Ru(2)−C(4) | 2.08(1) | Ru(3)−C(3) | 1.82(1) |
| Ru(3)−C(4) | 2.15(1) | Ru(1)−O(5) | 2.084(7) |
| Ru(2)−O(5) | 2.072(7) | Ru(3)−O(5) | 2.083(8) |
| C(1)−O(1) | 1.17(2) | C(2)−O(2) | 1.17(1) |
| C(3)−O(3) | 1.16(2) | C(4)−O(4) | 1.24(1) |
| Ru(2)−Ru(1)−Ru(3) | 60.41(4) | Ru(1)−Ru(2)−Ru(3) | 59.90(4) |
| Ru(1)−Ru(3)−Ru(2) | 59.68(4) | Ru(2)−Ru(1)−P(1) | 95.88(9) |
| Ru(2)−Ru(1)−P(6) | 144.14(10) | Ru(3)−Ru(1)−P(1) | 138.66(9) |
| Ru(3)−Ru(1)−P(6) | 85.74(10) | Ru(1)−Ru(2)−P(2) | 89.24(8) |
| Ru(1)−Ru(2)−P(3) | 138.53(9) | Ru(3)−Ru(2)−P(2) | 145.64(9) |
| Ru(3)−Ru(2)−P(3) | 94.9(1) | Ru(1)−Ru(3)−P(4) | 145.6(1) |
| Ru(1)−Ru(3)−P(5) | 96.2(1) | Ru(2)−Ru(3)−P(4) | 89.0(1) |
| Ru(2)−Ru(3)−P(5) | 138.3(1) | Ru(2)−Ru(1)−C(1) | 118.2(4) |
| Ru(2)−Ru(1)−C(4) | 49.1(3) | Ru(3)−Ru(1)−C(1) | 125.6(5) |
| Ru(3)−Ru(1)−C(4) | 51.0(3) | Ru(1)−Ru(2)−C(2) | 121.7(4) |
| Ru(1)−Ru(2)−C(4) | 49.2(3) | Ru(3)−Ru(2)−C(2) | 120.2(5) |
| Ru(3)−Ru(2)−C(4) | 50.7(3) | Ru(1)−Ru(3)−C(3) | 118.5(4) |
| Ru(1)−Ru(3)−C(4) | 48.7(3) | Ru(2)−Ru(3)−C(3) | 121.4(4) |
| Ru(2)−Ru(3)−C(4) | 48.4(3) | Ru(2)−Ru(1)−O(5) | 48.81(18) |
| Ru(3)−Ru(1)−O(5) | 49.0(2) | Ru(1)−Ru(2)−O(5) | 49.2(2) |
| Ru(3)−Ru(2)−O(5) | 48.8(2) | Ru(1)−Ru(3)−O(5) | 49.0(2) |
| Ru(2)−Ru(3)−O(5) | 48.4(2) | P(1)−Ru(1)−P(6) | 103.4(1) |
| P(2)−Ru(2)−P(3) | 100.2(1) | P(4)−Ru(3)−P(5) | 99.3(1) |
| P(1)−Ru(1)−C(1) | 95.0(5) | P(1)−Ru(1)−C(4) | 137.8(4) |
| P(6)−Ru(1)−C(1) | 90.2(4) | P(6)−Ru(1)−C(4) | 118.8(4) |
| P(2)−Ru(2)−C(2) | 87.7(5) | P(2)−Ru(2)−C(4) | 120.9(4) |
| P(3)−Ru(2)−C(2) | 99.1(4) | P(3)−Ru(2)−C(4) | 138.9(4) |
| P(4)−Ru(3)−C(3) | 88.9(4) | P(4)−Ru(3)−C(4) | 121.2(3) |
| P(5)−Ru(3)−C(3) | 99.7(4) | P(5)−Ru(3)−C(4) | 139.4(3) |
| P(1)−Ru(1)−O(5) | 89.7(2) | P(6)−Ru(1)−O(5) | 100.8(2) |
| P(2)−Ru(2)−O(5) | 100.4(2) | P(3)−Ru(2)−O(5) | 89.4(2) |
| P(4)−Ru(3)−O(5) | 100.3(2) | P(5)−Ru(3)−O(5) | 89.9(2) |
| C(1)−Ru(1)−O(5) | 166.7(4) | C(4)−Ru(1)−O(5) | 82.4(4) |
| C(2)−Ru(2)−O(5) | 167.1(5) | C(4)−Ru(2)−O(5) | 82.8(4) |
| C(3)−Ru(3)−O(5) | 165.5(5) | C(4)−Ru(3)−O(5) | 80.8(4) |
| C(1)−Ru(1)−C(4) | 85.8(5) | C(2)−Ru(2)−C(4) | 84.4(5) |
| C(3)−Ru(3)−C(4) | 84.9(5) | Ru(1)−C(1)−O(1) | 177.2(11) |
| Ru(2)−C(2)−O(2) | 175(1) | Ru(3)−C(3)−O(3) | 176(1) |
| Ru(1)−C(4)−O(4) | 132.4(9) | Ru(2)−C(4)−O(4) | 133.0(8) |
| Ru(3)−C(4)−O(4) | 129(1) | Ru(1)−C(4)−Ru(2) | 81.8(5) |
| Ru(1)−C(4)−Ru(3) | 80.3(4) | Ru(2)−C(4)−Ru(3) | 80.9(4) |
| Ru(1)−O(5)−Ru(2) | 82.0(3) | Ru(1)−O(5)−Ru(3) | 82.0(3) |
| Ru(2)−O(5)−Ru(3) | 82.8(3) | | |

The arrangement of the $\mu$-dppm ligands in **3** is very unusual. In most complexes containing $M_3(\mu\text{-dppm})_3$ units, each $M_2PCP$ unit adopts an envelope conformation as shown in **A**, and the

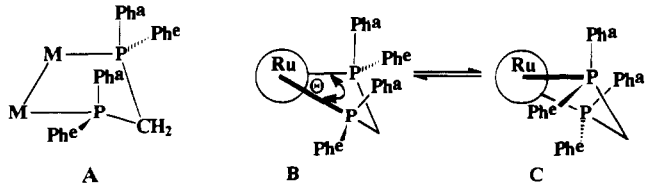


**A** **B** **C**

**a = axial, e = equatorial** **Projection down Ru-Ru bond**

phenyl groups on the same side as the $CH_2$ flap are then equatorial while those on the other side are axial.[9] If one side of the triangle contains a bulkier ligand than the other, two or three of the $CH_2$ flaps are directed *toward* the bulkier ligand so that most or all of the phenyl substituents on that side are equatorial and steric congestion is minimized, although at the expense of increased steric effects on the other side of the triangle.[9] In cluster **3** the two faces of the $Ru_3$ triangle are coordinated by four carbonyl ligands and one oxo ligand,

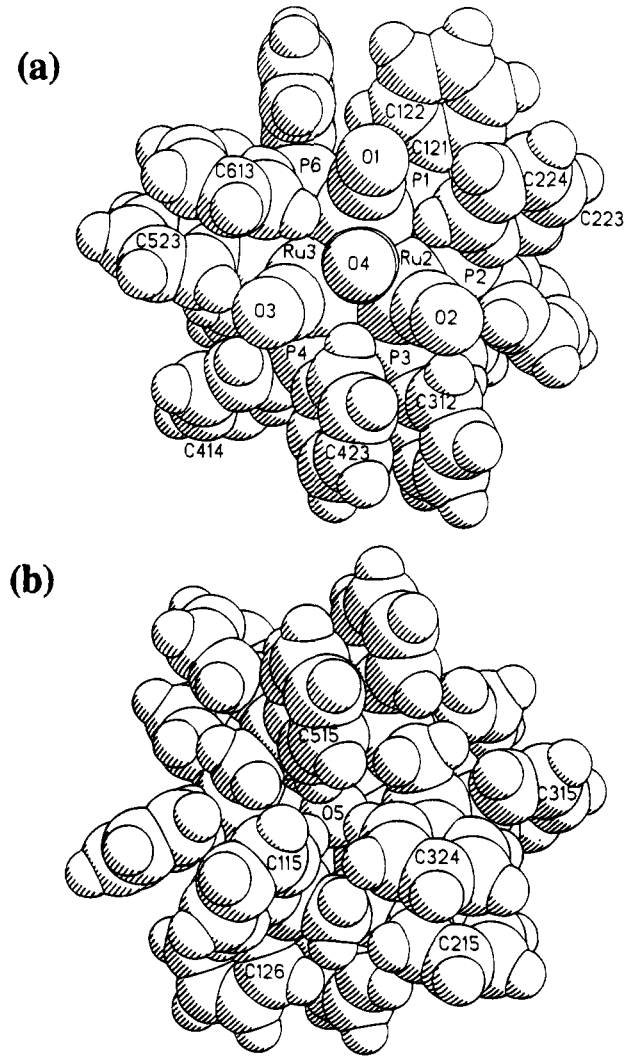


**Figure 2.** Space-filling models of the structure of **3**, showing views perpendicular to the $Ru_3$ plane (a) on the carbonyl side and (b) on the oxo side of the $Ru_3$ triangle.

respectively, and the four carbonyls obviously require a larger cavity. However, all $CH_2$ flaps in **3** are directed toward the $\mu_3$-O ligand, thus leading to equatorial phenyl groups on this side and axial phenyl groups on the carbonyl side. The apparent anomaly is rationalized as follows. The phosphorus atoms of the $\mu$-dppm ligands are displaced from the $Ru_3$ plane toward the $\mu_3$-O ligand. The distances of the phosphorus atoms from the $Ru_3$ plane are 1.368(4), 1.357(4), and 1.400(4) Å for P(1), P(3), and P(5) and 0.627(4), 0.588(4), and 0.489(4) Å for P(2), P(4), and P(6). The corresponding angles P(1)−Ru(1)−O(5), P(3)-Ru(2)−O(5), and P(5)−Ru(3)−O(5) are about 11° smaller than P(2)−Ru(2)−O(5), P(4)−Ru(3)−O(5), and P(6)−Ru(1)−O(5) (Table 1), and the dihedral angles PRuRuP for each $Ru_2(\mu\text{-dppm})$ group (see structure **B**) are in the range $\Theta = 20.0-23.9°$. The steric effects which result are illustrated in the space-filling diagrams in Figure 2, showing views perpendicular to the $Ru_3$ plane. On the carbonyl side, the axial phenyl groups

(8) Lavigne, G.; Lugan, N.; Bonnet, J. J. *New. J. Chem.* **1981**, *5*, 423.

(9) Puddephatt, R. J.; Manojlović-Muir, Lj.; Muir, K. W. *Polyhedron* **1990**, *9*, 2767. Slow conformational equilibration is known in some binuclear complexes such as $[Pt_2Cl(PPh_3)(\mu\text{-dppm})_2]^+$, where the bulky $PPh_3$ group is responsible: Blau, R. J.; Espenson, J. H.; Kim, S.; Jacobson, R. A. *Inorg. Chem.* **1986**, *25*, 757. Of course, the general phenomenon of restricted rotation in clusters is well established. See, for example: Einstein, F. W. B.; Johnston, V. J.; Ma, A. K.; Pomeroy, R. K. *Organometallics* **1990**, *9*, 52.

on P(2), P(4), and P(6), which lie closer to the $Ru_3$ plane, are of greatest concern, but they are oriented between pairs of terminal carbonyl ligands and so short nonbonded contacts are avoided. Although the phenyl groups on the oxo side of the $Ru_3$ triangle are equatorial, the displacement of phosphorus atoms to this side leads to greater steric congestion (Figure 2). In particular, the phenyl substituents on P(1), P(3), and P(5) lie over the $\mu_3$-O ligand and give rise to relatively short nonbonded distances between the oxo ligand and the *ortho*-hydrogens: O(5)···H(116), 2.31; O(5)···H(326), 2.35; O(5)···H(516), 2.43 Å. The oxo ligand is protected from external attack, except by the smallest reagents, by this shell of phenyl substituents. The cluster has approximate $C_3$ symmetry with twisted dppm ligands and so is naturally chiral, but the crystal contains equal numbers of the two enantiomers.

**Mechanism of the Formation of 3.** Cluster **3** is formed slowly (several days) by reaction of **1** with $AgO_2CCF_3$ in the presence of air, but no reaction occurs in the absence of air. Under these conditions, therefore, the $\mu_3$-O ligand is derived from oxygen from the air. Several other metal complexes "catalyze" the oxidation reaction. Thus **3** has been obtained by reaction of **1** in the presence of air with the reagents $[Cu(CNMe)_4][BF_4]$, $[Pt(O_2CCF_3)_2(dppm)]$, $[Ph_3PAuCl]$, $CoCl_2{\cdot}6H_2O$, and $FeCl_2{\cdot}6H_2O$. Cluster **1** is inert to reaction with $O_2$ alone; for example, it can be refluxed in benzene or 2-ethoxyethanol under $O_2$ without any decomposition and so it is clear that the metal ions are needed as coreagents. In a similar way, trimethylamine *N*-oxide gives no detectable reaction with **1** after 1 day at room temperature, but reaction to give **3** is complete in 1 day in the presence of silver(I), thus giving rise to the most convenient synthetic method for **3**.

The reaction of **1** to give **3** is most simply given by eq 1, where [O] is donated by an oxygen atom donor, $O_2$ or $Me_3NO$ as is common in the formation of oxo complexes.[5] As well as

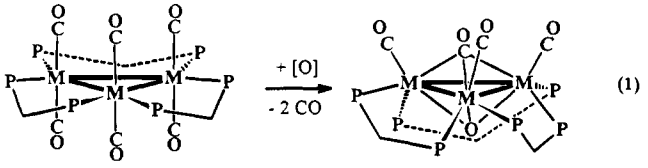


(1)

the oxygen atom addition, two carbonyl ligands are lost and one moves from one side of the $Ru_3$ triangle to the other (and must presumably dissociate and then recombine in order to do this) in converting **1** to **3**. We note that **1** is very inert to carbonyl dissociation since Ru−CO back-bonding is strong in the electron-rich cluster. Equation 1 is clearly oversimplified because it does not indicate the involvement and reduction of silver(I) in the formation of **3**. $Me_3NO$ may contribute both as an oxygen atom donor and by abstraction of one or more carbonyl ligands from **1** by conversion to $CO_2$. It is likely that reaction is initiated by reversible electron transfer from the electron-rich **1** to $Ag^+$, giving the cation radical $\mathbf{1}^+$, which then undergoes CO dissociation and oxygen atom transfer from $O_2$ or $Me_3NO$ and, at some stage, reduction back to the neutral product. The metal reagent may be expected to be a catalyst in this sense. Since no intermediates could be detected, the detailed mechanism could not be determined. There is a close analogy to the formation of **3** in the oxidation by air of $[Ru_3(CO)_8(\mu\text{-dppm})_2]$, **4**, to give $[Ru_3(\mu_3\text{-O})(CO)_6(\mu\text{-dppm})_2]$, **6**.[8] This reaction occurs thermally in the absence of other reagents and differs from the formation of **3** in this respect: It is known that **4** adds electrophiles, including silver(I), to the unbridged Ru−Ru bond, whereas complex **1** can add only the proton in this way since steric hindrance prevents the approach of larger electrophiles.[10] The higher reactivity of **4** compared to **1** toward $O_2$ could also be due to steric hindrance in **1**, but if reaction is initiated by carbonyl dissociation, it could also be due to **1** being more inert to loss of CO. Hence both an oxygen atom donor and a co-oxidant appear necessary for the efficient formation of **3** from **1**.

**A Protonation Reaction and Other Properties of 3.** In general, cluster **3** is remarkably stable and unreactive. For example, it undergoes thermal decomposition only at about 360 °C, as studied by DSC and TGA. It fails to react with reagents such as MeI, HCCH, and $H_2$ or with electrophiles such as $Ag^+$ and $Ph_3PAu^+$. These properties are rationalized in terms of the structure (Figure 2), in which the metal−metal bonds and oxo ligand are both protected from attack by the shell of phenyl substituents of the dppm ligands. In contrast, complex **6** reacts with $H_2$ to give $[Ru_3(\mu_3\text{-O})(\mu\text{-H})_2(CO)_5(\mu\text{-dppm})_3]$, **7**, which adds several electrophiles $E^+ = H^+$, $Ag^+$, and $Ph_3PAu^+$ to give $[Ru_3(\mu\text{-E})(\mu_3\text{-O})(\mu\text{-H})_2(CO)_5(\mu\text{-dppm})_3]^+$, **8**, by addition to the unbridged Ru−Ru bond.[11] Only the proton reacts with the more sterically hindered complex **3** as outlined below.

The contrast between reactions of **7** and **3** with protic reagents is illustrated in eqs 2 and 3. Complex **3** reacts reversibly with

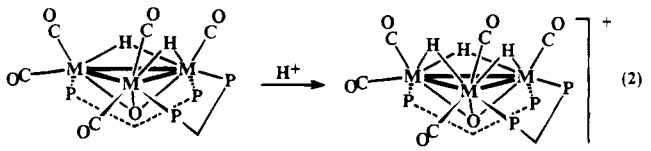


(2)

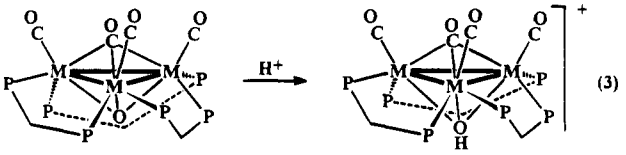


(3)

HCl to give **9** according to eq 3 by protonation of the $\mu_3$-O ligand instead of a Ru−Ru bond. Attempts to recrystallize **9** often led to loss of the proton with formation of **3**, but **9** was characterized in solution as the chloride salt and could be isolated as the chloride, hexafluorophosphate, and tetraphenylborate salt. Of these, the hexafluorophosphate appeared least prone to deprotonation to give **3**. The proton addition and loss were easily reversible: thus addition of base to a solution of **9** gave back **3** as monitored by $^{31}P$ NMR spectroscopy. However, a solution containing both **3** and **9** gave separate resonances for the two species, showing that proton exchange is slow on the NMR time scale (Figure 3). Complex **9** could also be prepared by the oxidation of $[Ru_3(\mu\text{-H})(CO)_6(\mu\text{-dppm})_3]^+$ with silver(I) and $O_2$.

**Spectroscopic Properties and Fluxionality of 3 and 9.** Most of the spectroscopic data for **3** and **9** are as expected and require little discussion. For example, the IR spectrum of **3** contains bands due to $\nu$(CO) at 1925 (vs), 1909 (vs) $cm^{-1}$ for the terminal carbonyl ligands and at 1627 (s) $cm^{-1}$ for the bridging carbonyl ligand. The terminal carbonyl bands shifted to higher frequency in the cationic cluster **9** as expected, but the frequency for the $\mu_3$-CO ligand was unchanged. The FAB mass spectra of both **3** and **9** contained envelopes of peaks corresponding to the mass ion. In each case, the $^1H$ NMR spectra contained two multiplets assigned to the $CH^aH^bP_2$ protons. For **9** the OH resonance was identified at $\delta = 9.04$ in $CD_2Cl_2$, appearing as a sharp singlet; there was no resonance in the region expected for a metal hydride ($\delta = 0$ to $-40$).

(10) Ladd, J. A.; Hope, H.; Balch, A. L. *Organometallics* **1984**, *3*, 1838.
(11) Colombie, A.; Bonnet, J. J.; Fompeyrine, P.; Lavigne, G.; Sunshine, S. *Organometallics* **1986**, *5*, 1154.

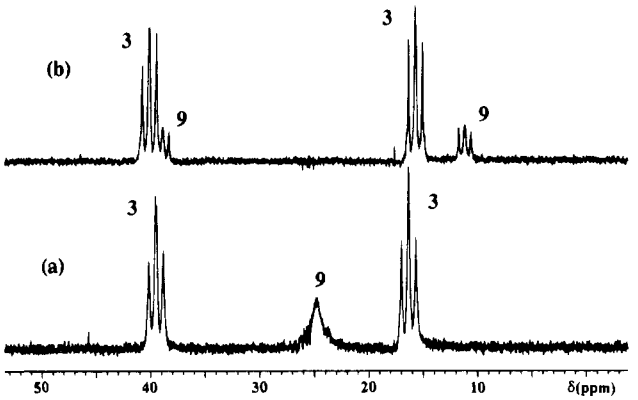


**Figure 3.** $^{31}P$ NMR spectra of a mixture of **3** and **9** in $CD_2Cl_2$: (a) at 22 °C; (b) at −80 °C. Note that **9** is fluxional at room temperature but **3** is not, and this is also true in samples where only pure **3** or **9** is present.

**Scheme 1**

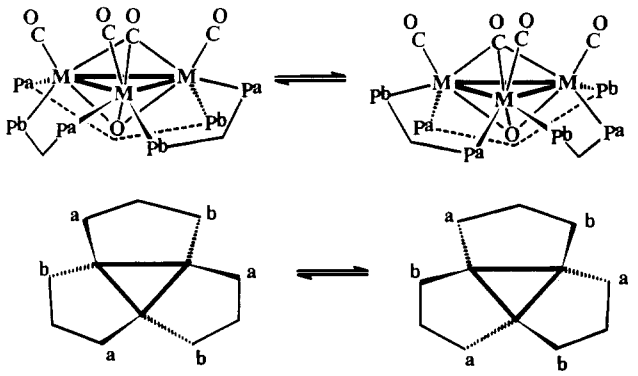

The above data are all consistent with **3** and **9** having a $M_3(\mu\text{-dppm})_3$ core with $C_{3v}$ symmetry. However, the $^{31}P$ NMR spectrum of **3** contained *two* multiplet resonances at $\delta = 16$ and 39, indicating lower symmetry. In a large number of $M_3(dppm)_3$ clusters studied previously, there are examples giving one, three, and six $^{31}P$ resonances as the symmetry is lowered by the presence of other ligands but, as far as we are aware, none giving two resonances.[9] The spectrum of **3** is interpreted in terms of the structure shown in Figure 1, with approximate $C_3$ symmetry, in which the phosphorus atoms are grouped in two sets P(1),P(3),P(5) and P(2),P(4),P(6) according to the extent of displacement from the $Ru_3$ plane. Steric congestion then prevents easy exchange between the two environments. The fluxional process was studied by using variable-temperature NMR spectroscopy. For complex **3**, separate $^{31}P$ signals were still clearly resolved in $C_6D_6$ at 75 °C although some broadening occurred. In 1,1,2,2-tetrachloroethane, the signals broadened and then coalesced at about 100 °C, but with some thermal decomposition at this temperature. Complex **3** was more stable in dmso-$d_6$, and coalescence was observed only at 200 °C. The apparent activation energies for fluxionality are calculated to be 65 and 83 kJ $mol^{-1}$ for solvents $C_2H_2Cl_4$ and dmso, respectively. The large solvent dependence is unusual, and the value in dmso is considered more reliable since impurities from the decomposition might affect the reaction in tetrachloroethane. The interconversion of the $P^a$ and $P^b$ environments is depicted in Scheme 1. Each $Ru_2(\mu\text{-dppm})$ group must undergo the libration **B** ⇌ **C**, and all three such groups probably librate in a concerted fashion to give the overall effect of eq 1; in the transition state, the six phosphorus atoms are probably approximately coplanar (i.e. Θ in **B** = 0 for all three dppm groups).

Complex **9** gives similar NMR properties at low temperature, but fluxionality is much easier (Figure 3). Thus the coalescence temperature in $CD_2Cl_2$ is *ca.* 5 °C and the activation energy is estimated to be only 47 kJ $mol^{-1}$. A possible explanation is that the Ru−Ru bonds are somewhat longer in **9** than in **3**, thus leading to lower steric congestion and so easier rearrangement. We have been unable to grow crystals of **9** in order to check this hypothesis. The fluxional process established for **3** and **9** appears to be unprecedented in dppm complex chemistry.[9]

## Experimental Section

**Synthesis of $[Ru_3(\mu_3\text{-O})(\mu_3\text{-CO})(CO)_3(\mu\text{-dppm})_3]$, 3.** To a stirring solution of $[Ru_3(CO)_6(\mu\text{-dppm})_3]$ (0.3g, 0.12 mmol) in $CH_2Cl_2$ (20 mL) were added $AgO_2CCF_3$ (0.01g, 0.12 mmol) and then $Me_3NO$ (0.02 g, 0.18 mmol). The mixture was stirred for 16 h in the dark. The original red color of the solution changed to orange with formation of silver metal. The mixture was then filtered, and the solvent was removed under vacuum. The orange solid was redissolved in $CH_2Cl_2$ (5−6 mL) and the solution chromatographed through a column of neutral alumina using ether as eluent. Fractions containing **3** were combined, the solvent was removed under vacuum, and the product was recrystallized from $CH_2Cl_2$/EtOH. Yield: 50%. Mp: 360 °C dec. Anal. Calc for $C_{79}H_{66}O_5P_6Ru_3 \cdot 0.5CH_2Cl_2$: C, 58.6; H, 4.1. Found: C, 58.9; H, 4.5. IR (Nujol): $\nu$(CO) = 1925 (vs), 1909 (vs), 1627 (s) $cm^{-1}$. FAB-MS: $m/z$ = 1584. NMR ($CD_2Cl_2$): $\delta(^1H)$ = 3.07 [m, 3H, $CH_2$], 3.58 [m, 3H, $CH_2$]; $\delta(^{31}P)$ = 39 [m, 3P, dppm], 16 [m, 3P, dppm].

**Synthesis of $[Ru_3(\mu_3\text{-OH})(\mu_3\text{-CO})(CO)_3(\mu\text{-dppm})_3]X$ ($X = Cl^-, PF_6^-, BPh_4^-$).** To a solution of **3** (0.04g, 0.025 mmol) in $CH_2Cl_2$ (5 mL) was added HCl (0.05 mL, 7 M), and the mixture was shaken for 5 min. The solvent was removed to give the product $[Ru_3(OH)(CO)_4(dppm)_3]Cl$. Yield: 0.04 g. Anal. Calc for $C_{79}H_{67}ClO_5P_6Ru_3 \cdot 1.5CH_2Cl_2$; C, 55.3; H, 4.0. Found: C, 55.1; H, 3.8. IR (Nujol): 1955 (s), 1930 (vs), 1913 (s), 1626 (m) $cm^{-1}$. FAB-MS: $m/z$ = 1585. NMR ($CD_2Cl_2$): $\delta(^1H)$ = 3.1 [m, 3H, $CH_2$], 4.1 [m, 3H, $CH_2$], 9.0 [s, 1H, OH]; $\delta(^{31}P)$ at 22 °C = 25 [br s, dppm]. $\delta(^{31}P)$ at −80 °C = 11 [m, 3P, dppm], 38 [m, 3P, dppm].

The $PF_6^-$ and $BPh_4^-$ salts were prepared by reaction of $[Ru_3(OH)(CO)_4(dppm)_3]Cl$ in $CH_2Cl_2$ with $NH_4PF_6$ or $NaBPh_4$ in ethanol. The solvent was removed, and the product was extracted using $CH_2Cl_2$. The NMR properties were as for the chloride salt.

**X-ray Structure Determination.** Single crystals of **3** were grown by diffusion of ethanol into a solution in 1,2−dichloroethane. A crystal with dimensions 0.19 × 018 × 0.38 mm was coated with paraffin oil and flame-sealed in a capillary tube. The data collection was carried out using an Enraf-Nonius CAD4F diffractometer and Cu Kα radiation[12] with a nickel filter at 23 °C. Photoindexing and automatic indexing routines, followed by least squares fits of 21 accurately centered reflections (54.0 ≤ 2θ ≤ 67.6°), gave cell constants and an orientation matrix. Intensity data were recorded in $\omega-2\theta$ mode, at variable scan speeds (0.824−4.12° $min^{-1}$) and a scan width of (0.75 + 0.14 tan θ)°, with a maximum time per datum of 60 s. Static background measurements were made at the end points of the width (0.85 + 0.14 tan θ)°. Three standard reflections were monitored every 180 min of X-ray exposure time. In all, 10 766 reflections in the 2θ range 0−110° (−21 ≤ $h$ ≤ 21, −1 ≤ $k$ ≤ 31, −1 ≤ $l$ ≤ 13) and 55 repetitions of the standards were recorded. The NRCVAX crystal structure programs[13] running on a SUN 3/80 workstation were used for processing

(12) *CAD4 Diffractometer Manual*; Enraf-Nonius: Delft, The Netherlands, 1988.
(13) Gabe, E. J.; Le Page, Y.; Charland, J.-P.; Lee, F. C. *J. Appl. Crystallogr.* **1989**, *22*, 384.

**Table 2.** Crystal Data and Experimental Details for **3**

| | |
|---|---|
| formula | $C_{79}H_{66}O_5P_6Ru_3 \cdot 0.8C_2H_4Cl_2 \cdot 0.8C_2H_5OH$ |
| fw | 1676.79 |
| crystal system, space group | monoclinic, $P2_1/n$ |
| cell dimensions | $a = 19.771(2)$ Å |
| | $b = 29.711(2)$ Å |
| | $c = 13.007(2)$ Å |
| | $\beta = 94.01(9)°$ |
| temperature, °C | 23 |
| cell volume, Å$^3$; $Z$ | 7622(1); 4 |
| density, g·cm$^{-3}$: obsd, calcd | 1.48, 1.461 |
| radiation; wavelength, Å | Cu Kα; 1.541 84 |
| abs coeff, cm$^{-1}$ | 64.3 |
| no. of observns, variables | 6264 ($I \geq 2.5\sigma(I)$), 358 |
| final model:[a] $R_F$, and $R_{wF}$ | 0.063, 0.045 |
| GOF[b] | 2.57 |

[a] $R_F = \Sigma||F_o| - |F_c||/\Sigma|F_o|$; $R_{wF} = [\Sigma w(|F_o| - |F_c|)^2/\Sigma w|F_o|^2]^{1/2}$. [b] GOF $= \Sigma w(|F_o| - |F_c|)^2/$(no. of reflns − no. of params)$^{1/2}$.

the data, solution and refinement of the structure. A Gaussian absorption correction was made using the routine ABSORP after indexing the faces of the data crystal. The maximum and minimum transmission values are 0.4198 and 0.2511, respectively. The cell parameters and systematic absences[14] indicated the space group $P2_1/n$, and this was confirmed by successful solution and refinement of the structure. The symmetry-equivalent reflections were averaged ($R_F = 0.025$), leaving 9495 unique reflections. The structure refinements were done by full-matrix least squares techniques on $F$. Anisotropic thermal parameters were assigned for all Ru, P, O, and carbonyl carbon atoms and were refined. The phenyl rings were constrained to a regular hexagon with C−C = 1.395 Å. All hydrogen atoms were placed in ideal positions (C−H = 1.08 Å), and their thermal parameters were allowed to ride 10% more on the attached carbon atoms. The solvent molecules dichloroethane and ethanol were found in the difference Fourier syntheses. The occupancies of these solvent molecules were refined to 0.8. Hydrogen atoms were included in their ideal positions for dichloroethane, and the chlorine atoms were refined anisotropically in the least squares cycles. In the final cycles, for 358 variables and 6264 ($I \geq 2.5\sigma(I)$) observations, the model converged at $R_F = 0.063$, $R_{wF} = 0.045$, and GOF = 2.57 based on counting statistics. Crystal data are given in Table 2, and selected atomic positional parameters, in Table 3.

(14) *International Tables for X-ray Crystallography*; D. Reidel Publishing Co.: Boston, 1983; Vol. A.

**Table 3.** Selected Atomic Positional and Thermal Parameters

| atom | $x$ | $y$ | $z$ | $B_{iso}$, Å$^2$ |
|---|---|---|---|---|
| Ru(1) | 0.18223(4) | 0.15466(3) | 0.82128(9) | 2.73(5) |
| Ru(2) | 0.31923(4) | 0.14925(3) | 0.86134(9) | 2.78(5) |
| Ru(3) | 0.23386(5) | 0.12660(3) | 1.01094(9) | 2.72(5) |
| P(1) | 0.18184(16) | 0.13168(11) | 0.6490(3) | 3.19(18) |
| P(2) | 0.33219(15) | 0.15288(12) | 0.6877(3) | 3.28(19) |
| P(3) | 0.40219(15) | 0.09395(11) | 0.9109(3) | 3.16(19) |
| P(4) | 0.32266(15) | 0.09268(11) | 1.1008(3) | 3.06(18) |
| P(5) | 0.14778(16) | 0.07258(11) | 1.0370(3) | 3.07(19) |
| P(6) | 0.07991(15) | 0.12940(11) | 0.8712(3) | 3.20(19) |
| C(1) | 0.1454(6) | 0.2094(4) | 0.7920(12) | 3.9(8) |
| C(2) | 0.3719(6) | 0.1994(4) | 0.8757(12) | 3.7(8) |
| C(3) | 0.2237(7) | 0.1629(4) | 1.1214(11) | 3.8(8) |
| C(4) | 0.2470(5) | 0.1885(4) | 0.9285(10) | 2.9(7) |
| O(1) | 0.1243(4) | 0.2455(3) | 0.7746(9) | 5.8(6) |
| O(2) | 0.4011(4) | 0.2335(3) | 0.8858(8) | 5.7(6) |
| O(3) | 0.2202(5) | 0.1875(3) | 1.1899(8) | 5.5(6) |
| O(4) | 0.2476(4) | 0.2278(3) | 0.9618(7) | 3.8(5) |
| O(5) | 0.2446(3) | 0.1004(4) | 0.8645(6) | 2.5(4) |
| C(10) | 0.2683(5) | 0.1185(4) | 0.6141(9) | 3.0(3) |
| C(20) | 0.3705(5) | 0.0587(4) | 1.0142(9) | 2.7(3) |
| C(30) | 0.0891(5) | 0.0722(4) | 0.9204(9) | 2.6(3) |

**Acknowledgment.** We thank the NSERC (Canada) for financial support and Dr. N. C. Payne for X-ray and computing facilities.

**Supporting Information Available:** Tables S1−S6, giving atomic positional and thermal parameters, bond distances and angles, anisotropic thermal parameters, calculated H atom coordinates, weighted least squares planes and dihedral angles, and selected torsion angles (16 pages). Ordering information is given on any current masthead page.

IC941439T